Supplemental Content to

Hydraulic Fracturing Shear/Tensile/Compressive Crack Investigation Using Microseismic Data

By Han Li, Xu Chang and Jinlai Hao

This supplemental content contains three figures listing the raw observed waveforms and inversion uncertainty analysis for the selected events A11 and C03 (Figure 3a–3c), and three tables listing the determined focal mechanisms of microseismic events in three HF stages using the DC, GD, and MT source models.

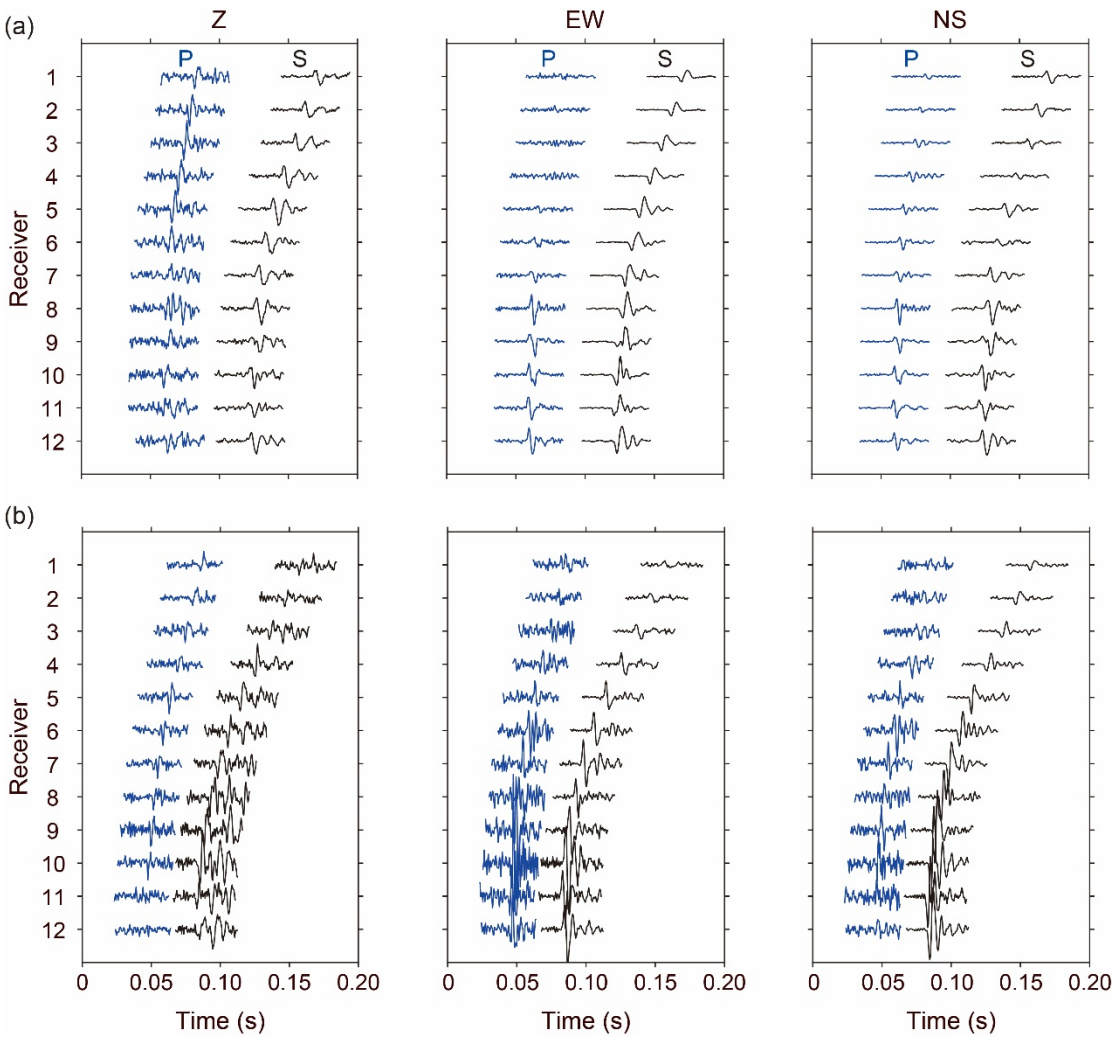


Figure S1. Raw observed waveforms for the selected events A11 (a) and C03 (b), whose locations are shown in Figure 3a–3c. The black and blue lines indicate the P and S velocity records, which are normalized with respect to the P and S amplitudes at receiver 5 for event A11 and receiver 8 for event C03, respectively.

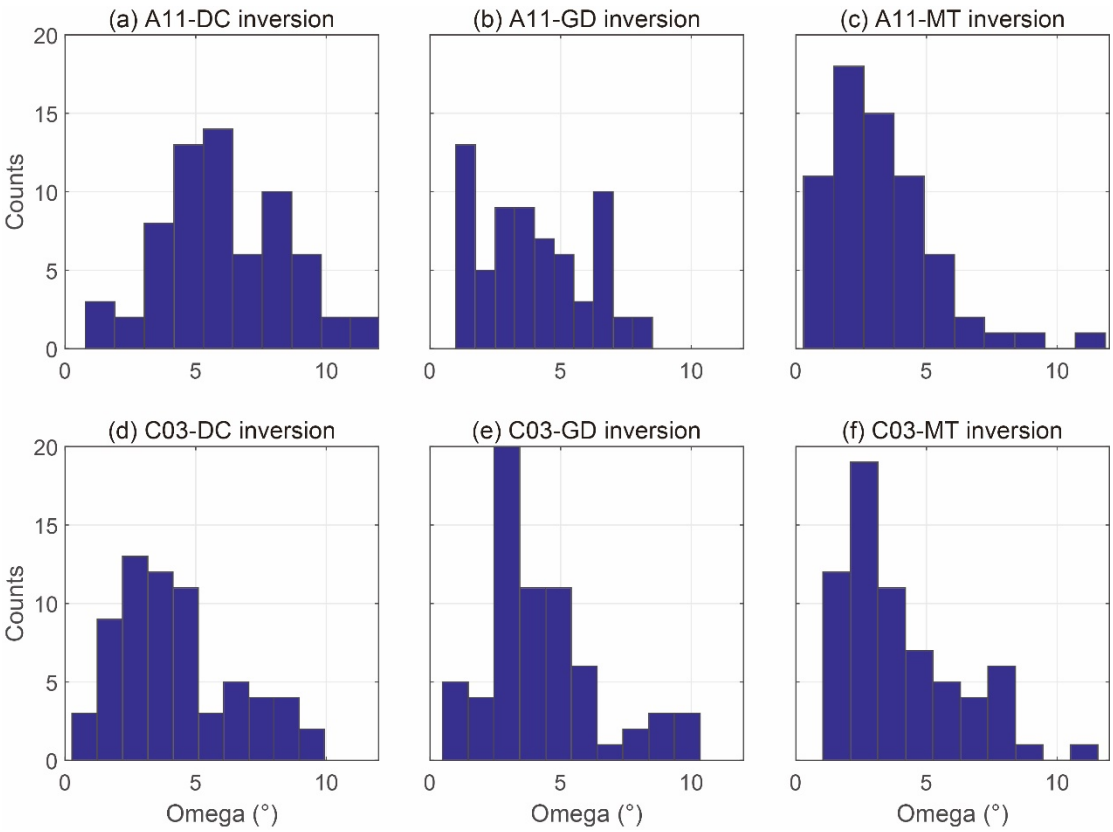


Figure S2. Bootstrap uncertainty analysis of the focal mechanism inversions for events A11 (a–c) and C03 (d–f), whose locations are shown in Figure 3a–3c. For each event, we use waveform data at 10 receivers from the total 12 receivers to perform inversions (the total count number is $C_{12}^{10} = 66$). The x label is the omega angle [1,2], which indicates the deviation in the orientations of the principal axis between the inversion results using data at 10 and 12 receivers.

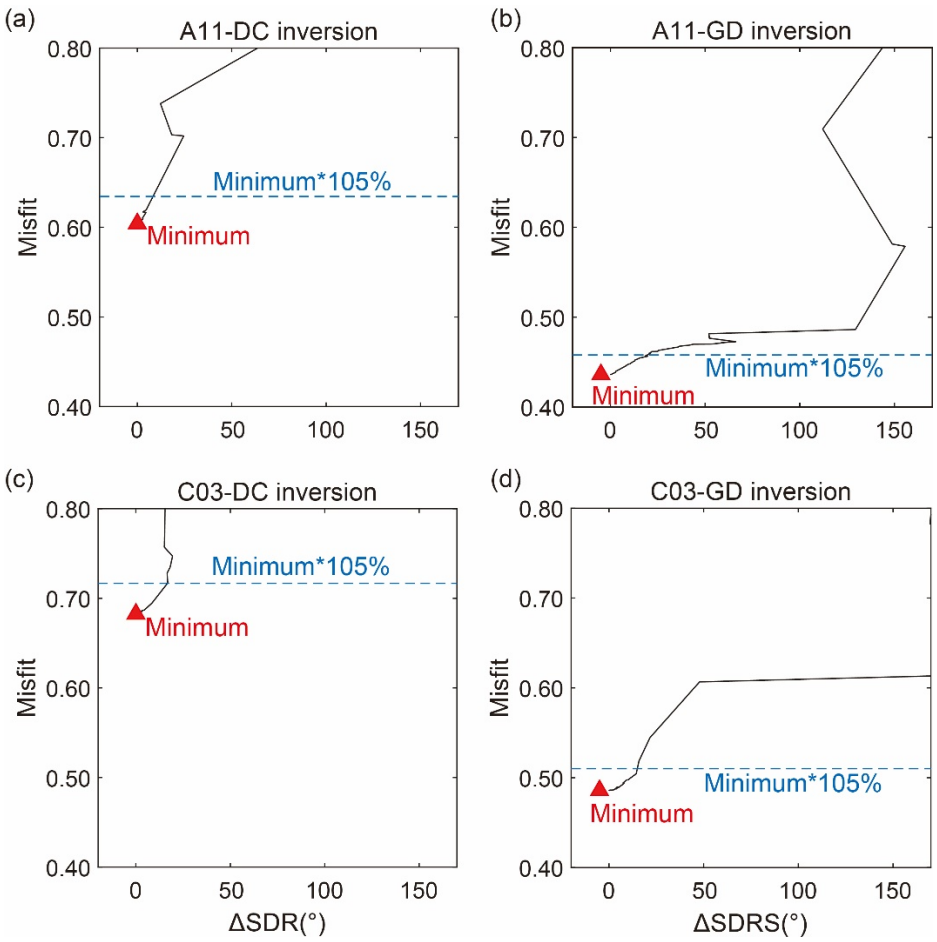


Figure S3. Uncertainty ranges of the DC and GD focal mechanism inversions using the fast simulated annealing algorithm for events A11 (a–b) and C03 (c–d), whose locations are shown in Figure 3a–3c. $\Delta\mathrm{SDR} = |\Delta\varphi| + |\Delta\delta| + |\Delta\lambda|$, where $|\Delta\varphi|$, $|\Delta\delta|$, and $|\Delta\lambda|$ denote the differences of the strike, dip, and rake angles from the output results (the angles with the minimum misfit), e.g., $|\Delta\varphi| = |\varphi - \varphi^{\mathrm{output}}|$. $\Delta\mathrm{SDRS} = \Delta\mathrm{SDR} + |\Delta\alpha|$, where α denotes the slope angle.

Table S1. Focal mechanism inversion results using the DC, GD, and MT models for 11 events in HF stage 1.

ID	Model	Nodal plane I			Nodal plane II			Components			Slope	Moment magnitude	VR	Quality
		Strike (°)	Dip (°)	Rake (°)	Strike (°)	Dip (°)	Rake (°)	DC (%)	CLVD (%)	ISO (%)	(°)		(%)	
A01	1-DC	261	45	–106	104	47	–73	100	0	0	-	–1.0	37	C
	2-GD	204	79	177	53	83	–32	7	41	52	56	–1.0	64	B
	3-MT	184	69	–164	89	76	–22	9	23	68	-	–0.8	73	A
A02	1-DC	182	54	37	81	76	143	100	0	0	-	–1.1	7	C
	2-GD	214	88	–23	356	77	168	10	40	50	49	–1.0	63	B
	3-MT	236	75	–24	333	67	–163	10	37	53	-	–0.8	67	B
A03	1-DC	233	76	–20	328	70	–160	100	0	0	-	–1.0	17	C
	2-GD	206	78	–2	239	79	–144	6	–42	–52	–58	–1.1	67	B
	3-MT	200	79	–14	292	77	–170	22	–5	–73	-	–0.9	73	A
A04	1-DC	221	68	21	131	90	158	100	0	0	-	–1.0	29	C
	2-GD	207	70	26	240	89	–144	8	–41	–51	–53	–1.1	75	A
	3-MT	193	78	–7	285	83	–168	43	–21	–36	-	–1.0	79	A
A05	1-DC	39	74	22	302	69	158	100	0	0	-	–0.6	–54	C
	2-GD	189	82	–11	195	80	–109	1	–44	–55	–84	–0.8	67	B
	3-MT	158	63	22	58	70	151	4	–15	–81	-	–0.5	79	A

A06	1-DC	47	87	12	316	78	168	100	0	0	-	–0.7	–37	C
	2-GD	214	73	22	217	75	25	0	–44	–56	–87	–1.0	69	B
	3-MT	215	76	–25	312	66	–164	22	70	8	-	–0.7	78	A
A07	1-DC	234	78	–18	327	72	–162	100	0	0	-	–1.1	49	C
	2-GD	211	84	–28	270	63	–156	25	–33	–42	–30	–1.1	77	A
	3-MT	209	83	–27	303	64	–172	46	–3	–51	-	–1.0	83	A
A08	1-DC	228	83	–11	321	78	–168	100	0	0	-	–1.1	44	C
	2-GD	214	88	–23	222	84	–21	1	–44	–55	–85	–1.2	63	B
	3-MT	175	65	42	64	52	148	13	–32	–55	-	–0.8	72	A
A09	1-DC	45	88	5	314	79	175	100	0	0	-	–1.0	35	C
	2-GD	199	75	–23	230	90	–152	7	–41	–52	–56	–1.1	63	B
	3-MT	211	79	–19	305	71	–169	52	37	–11	-	–1.1	69	B
A10	1-DC	230	86	–4	320	81	–176	100	0	0	-	–1.0	–15	C
	2-GD	184	84	48	29	71	–158	7	–41	–52	–55	–0.9	65	B
	3-MT	184	71	35	81	58	157	15	-6	–78	-	–0.9	74	A
A11	1-DC	221	88	–2	312	52	–178	100	0	0	-	–0.8	51	C
	2-GD	201	77	–21	256	80	–170	19	–36	–45	–36	–0.9	73	A
	3-MT	198	79	–22	293	69	–168	39	–6	–55	-	–0.8	77	A

Table S2. Focal mechanism inversion results using the DC, GD, and MT models for 11 events in HF stage 2.

ID	Model	Nodal plane I			Nodal plane II			Components			Slope	Moment magnitude	VR	Quality
		Strike (°)	Dip (°)	Rake (°)	Strike (°)	Dip (°)	Rake (°)	DC (%)	CLVD (%)	ISO (%)	(°)		(%)	
B01	1-DC	323	90	36	233	54	144	100	0	0	-	–1.2	35	C
	2-GD	205	90	–6	250	86	–176	12	–40	–49	–46	–1.2	71	A
	3-MT	187	78	1	97	89	168	8	–40	–52	-	–0.9	72	A
B02	1-DC	227	73	–22	324	69	–158	100	0	0	-	–0.8	1	C
	2-GD	209	74	4	238	78	–135	4	–43	–53	–62	–1.0	64	B
	3-MT	194	73	13	100	78	163	17	2	–82	-	–0.6	79	A
B03	1-DC	177	63	13	80	78	167	100	0	0	-	–1.1	–2	C
	2-GD	213	85	–21	358	81	177	8	41	51	52	–1.1	65	B
	3-MT	199	80	–9	290	81	–172	5	–8	87	-	–0.8	75	A
B04	1-DC	240	75	–11	333	80	–169	100	0	0	-	–1.0	60	B
	2-GD	216	81	18	89	81	175	21	–35	–44	–34	–0.9	72	A
	3-MT	204	80	3	113	84	170	19	–17	–64	-	–0.7	79	A
B05	1-DC	236	80	–18	329	72	–162	100	0	0	-	–1.0	34	C
	2-GD	210	85	–20	239	85	–178	5	–42	–53	–61	–1.0	65	B
	3-MT	184	65	29	81	64	152	6	–22	–72	-	–0.6	75	A

B06	1-DC	237	86	−10	328	80	−170	100	0	0	-	−1.1	62	B
	2-GD	237	86	−11	326	79	−176	95	−2	−3	−1	−1.1	62	B
	3-MT	218	86	−6	302	84	−176	21	−44	−35	-	−1.0	77	A
B07	1-DC	334	81	18	240	73	162	100	0	0	-	−1.1	56	C
	2-GD	248	89	15	216	81	165	6	42	52	57	−1.0	72	A
	3-MT	101	73	−18	196	72	−162	12	19	69	-	−0.8	78	A
B08	1-DC	48	90	−165	318	75	−15	100	0	0	-	−0.9	4	C
	2-GD	26	75	−65	194	79	−155	5	42	53	61	−0.9	81	A
	3-MT	54	52	−46	177	56	−132	5	25	71	-	−0.6	84	A
B09	1-DC	208	57	19	107	74	160	100	0	0	-	−1.2	13	C
	2-GD	230	84	44	206	74	−160	3	43	54	65	−1.2	61	B
	3-MT	253	84	−5	344	84	−174	16	26	58	-	−1.0	67	B
B10	1-DC	229	88	−2	320	58	−178	100	0	0	-	−0.9	37	C
	2-GD	205	82	19	61	85	173	8	−41	−51	−53	−0.9	60	B
	3-MT	180	66	29	77	64	153	6	−24	−70	-	−0.5	71	A
B11	1-DC	104	41	−180	14	90	−49	100	0	0	-	−1.1	44	C
	2-GD	218	85	−19	355	80	178	12	39	49	45	−0.9	61	B
	3-MT	245	66	−26	347	66	−154	5	42	54	-	−0.5	64	B

Table S3. Focal mechanism inversion results using the DC, GD, and MT models for 10 events in HF stage 3.

ID	Model	Nodal plane I			Nodal plane II			Components			Slope	Moment magnitude	VR	Quality
		Strike (°)	Dip (°)	Rake (°)	Strike (°)	Dip (°)	Rake (°)	DC (%)	CLVD (%)	ISO (%)	(°)		(%)	
C01	1-DC	105	70	–22	205	64	–157	100	0	0	-	–1.2	44	C
	2-GD	337	66	17	224	83	156	43	–25	–31	–18	–1.1	62	B
	3-MT	341	76	14	247	76	166	11	–50	–39	-	–0.8	62	B
C02	1-DC	236	70	11	142	79	169	100	0	0	-	–1.2	47	C
	2-GD	251	87	9	214	87	–180	8	41	51	53	–1.1	71	A
	3-MT	271	90	6	181	84	180	10	23	67	-	–0.9	77	A
C03	1-DC	323	90	19	233	71	161	100	0	0	-	–1.6	70	C
	2-GD	182	87	–3	242	86	–174	25	–33	–42	–30	–1.2	78	A
	3-MT	337	81	5	247	86	171	48	–15	–37	-	–1.1	82	A
C04	1-DC	134	74	–16	229	73	–164	100	0	0	-	–1.1	62	C
	2-GD	177	86	–3	241	85	–172	29	–32	–40	–27	–1.1	75	A
	3-MT	327	87	4	236	86	177	50	13	–37	-	–1.1	80	A
C05	1-DC	239	78	–16	333	74	–163	100	0	0	-	–1.3	63	C
	2-GD	231	84	–26	319	63	–175	78	–10	–12	–5	–1.2	68	B
	3-MT	222	85	–12	313	78	–175	40	–6	–55	-	–1.0	74	A

C06	1-DC	168	89	–9	258	81	–171	100	0	0	-	–0.8	65	C
	2-GD	268	77	–11	240	84	146	5	42	53	61	–0.6	84	A
	3-MT	165	83	–3	255	87	–173	14	–9	77	-	–0.4	87	A
C07	1-DC	278	73	78	134	21	102	100	0	0	-	–0.8	–4	C
	2-GD	240	87	–31	273	70	–147	7	–41	–52	–54	–0.6	66	B
	3-MT	52	84	14	320	76	174	6	–27	–67	-	–0.5	78	A
C08	1-DC	228	80	9	138	90	170	100	0	0	-	–1.3	47	C
	2-GD	205	83	10	235	89	–163	5	–42	–53	–59	–1.3	65	B
	3-MT	181	62	38	71	57	146	10	–44	–46	-	–1.0	72	A
C09	1-DC	236	78	–8	327	83	–172	100	0	0	-	–1.1	54	C
	2-GD	214	86	22	83	76	–173	17	–37	–46	–38	–1.1	60	B
	3-MT	199	73	28	100	63	161	11	–18	–71	-	–0.8	74	A
C10	1-DC	266	73	–16	1	75	–164	100	0	0	-	–1.1	47	C
	2-GD	174	86	30	25	76	–168	7	–41	–51	–56	–1.0	71	A
	3-MT	158	60	33	49	62	144	7	–29	–63	-	–0.6	74	A

References

1. Tape, W.; Tape, C. Angle between Principal Axis Triples. *Geophys. J. Int.* **2012**, *191*, 813–831, doi:10.1111/j.1365-246X.2012.05658.x.
2. Tape, W.; Tape, C. A Uniform Parametrization of Moment Tensors. *Geophys. J. Int.* **2015**, *202*, 2074–2081, doi:10.1093/gji/ggv262.